Submitted to *Composites A: Applied Science and Manufacturing*

Graded Polymer Composites Using Twin Screw Extrusion: A Combinatorial Approach to Developing New Energetic Materials

Frederick M. Gallant[1,2]
Hugh A. Bruck[1*]
Suzanne Prickett[2]
Mario Cesarec[2]

[1] *Department of Mechanical Engineering, University of Maryland, College Park, MD 20742*
[2] *Naval Surface Warfare Center, Indian Head, MD*

Abstract

The development of new energetic materials is a time-consuming, laborious, and sometimes dangerous process. Batch approaches are most commonly used, especially for energetic materials consisting of polymer composites. Recently, a manufacturing technology known as Twin Screw Extrusion (TSE), has been demonstrated to increase the safety and affordability for manufacturing composite energetic materials. This technology is also ideally suited to manufacturing graded polymer composites through transient operating and/or feed conditions. In this paper, the TSE process is employed to fabricate graded polymer composites in a combinatorial approach for developing new energetic materials. Graded composite energetic materials with 79 to 87% solids loading of Ammonium Perchlorate are processed. The dependence of burning rate properties on the variation in composition was determined through strand burning tests. These results were compared with a conventional design of experiments approach using the Kowalski algorithm. The correlation of composition to properties over a range of compositions between the new combinatorial approach and the conventional design of experiments approach validates the use of TSE processing as a combinatorial approach to developing new energetic materials. Because the TSE process is used to manufacture both energetic and non-energetic composite materials, the combinatorial approach can also be applied to the development of new polymer composites for non-energetic applications.

* Corresponding Author: Assistant Professor, email: bruck@eng.umd.edu, phone: 301-405-8711, fax: 301-314-9477

I. Introduction

Composite materials are being fabricated for energetic applications using a very high solids loading of energetic particles (>70 wt.%), typically bound by an energetic polymer. These materials have primarily been processed using batch techniques. By varying the solids content, particle sizes, and particle distributions, combined with smaller volume fractions of additives, it is possible to create a variety of formulations that exhibit a wide range of energy release rates, impact sensitivity, and thermal sensitivity.

Recently, alternative processing techniques that have been conventionally used for inert composite material systems have been pursued for the fabrication of composite energetic materials. In particular, a continuous processing technique known as twin screw extrusion has been particularly attractive for increasing the safety and affordability of manufacturing composite energetic materials. This technique is fairly well understood for the processing of polymer blends and homogeneous composite materials in a steady state.

More recently, it has been shown that the technique of twin screw extrusion can be run in a transient state to produce controlled variations in material distribution resulting in graded polymer composites [1]. The evolution of the gradient architecture was predicted using convolution process models based on residence distributions. Because the TSE process can be used for both energetic and non-energetic composite materials, non-energetic analogs consisting of a thermoplastic elastomer and potassium chloride were used to safely study the transient operation of the TSE process for the production of graded composite energetic materials. It also provided the opportunity to

develop basic knowledge of the TSE process that could be used in the production of new non-energetic polymer composites for control and sensing applications.

In this paper, the technique of twin screw extrusion is pursued as a combinatorial approach to the processing of new composite energetic materials. Using the previously developed convolution process model, it is shown that controlled gradient architectures can be predicted and then produced. The composition of these gradient architectures are then characterized, and then correlated to the combustion properties determined using burning rate testing. These results are compared with a conventional approach to determining the compositional dependence of burning rates using batch processing of formulations determined using a Kowalski design-of-experiments algorithm.

I. Prediction of Gradient Architectures Fabricated Using Twin Screw Extrusion Processing

To predict gradient architectures, a new convolution process model has been developed for the Twin Screw Extrusion (TSE) process [1]. This model is derived from a *n*th order ideal mixing model, and is expressed as follows:

$$F(x) = \int_0^x \frac{a_x^n}{(n-1)!} \left((x-x') - x_d\right)^{n-1} e^{-a_x\left((x-x')-x_d\right)} H((x-x') - x_d) u(x') dx' \qquad (1)$$

Where x is a measurement parameter such as time or volume, $F(x)$ is a measured characteristic of the extrudate output from the TSE process such as optical properties, $u(x)$ is the feed input into the extruder, $H(x)$ is the Heaviside step function, and a_x and x_d are the shape factor and delay parameter respectively. The shape factor, delay parameter, and order of the mixing model can be determined by applying an impulse

input to the process, and then fitting experimental data to the following form of equation (1):

$$F(x) = \frac{a_x^n}{(n-1)!}\left(x - x_d\right)^{n-1} e^{-a_x\left(x-x_d\right)} H(x - x_d) \tag{2}$$

This form of the output from the TSE process is called the *Residence Distribution*. When the measurement parameter is time, it is known as the *Residence Time Distribution (RTD)*; when the parameter is volume it is known as the *Residence Volume Distribution (RVD)*. The shape factor and delay parameter for RTDs can be easily converted to the shape factor and delay parameter for RVDs using the following relationships:

$$v_d = Qt_d \tag{3a}$$

$$a_v = \frac{a}{Q} \tag{3b}$$

where Q is the volumetric throughput.

Once the shape factor, delay parameter, and order of the mixing model have been established, a variety of gradient architectures can be fabricated in the TSE process by varying the input, with the exact gradient predicted using equation (1) and the precise input conditions. In the combinatorial approach to developing new energetic materials, the precise input conditions will be chosen depending on the region of the material design space that is of interest for exploration. This will be discussed further in the next section.

II. Processing of Composite Energetic Materials with Compositional Gradients

III.a Experimental Apparatus

A unique facility has been assembled at the Naval Surface Warfare Center in Indian Head, MD (NAVSEAIHMD) to address the specific needs for processing energetic polymer composites in a TSE process [2]. The extruder employed in the facility was a Werner & Pfleiderer ZSK-40 (mm) featuring segmented and cantilevered screws. It has a process length to diameter (L/D) ratio of 28, which is similar to the one employed at the University of Maryland in a previous investigation on graded polymer composites [1]. The six barrels were temperature controlled by five temperature controllers. The extruder barrel featured open ports for introducing the two solids and an additional port for vacuum deaeration. Many of the barrels are bored to allow for the insertion of temperature and pressure sensors to measure the physical state of the propellant during processing. Five combined sensors were used in process-critical areas in the barrel and at the die. The 40-mm extruder features a hydraulically clamped die holder that operates similar to a door. This is a safety feature unique to this extruder, which causes the door to open should the die pressure exceed the clamping pressure, thus relieving the pressure instantly.

Four feed streams were required to produce gradient architectures using the combinatorial approach, while the conventional approach required an additional feed stream. Two of the feed streams were solid ingredients (three for the conventional approach), and the other two were blends of liquid ingredients. The solid ingredients were fed to the extruder using K-Tron models T-37 and T-20 loss-in-weight twin-screw and single-screw feeders respectively. More details of the feeding arrangements that were not essential to this investigation can be found in previous technical documents [3,4].

The extruder configuration, feeding locations, and screw design for the energetic propellant are illustrated in *Figure 1*. Binder ingredients were compounded first, and then the fillers were added mid-process to a homogenized binder. Since the HyTemp elastomer was not thermoplastic, but rather a partially cross-linked polymer that was theromoset to increase the cross-link density, much lower barrel temperatures are employed than for conventional thermoplastic elastomers in a TSE process. The extruder was deaerated by vacuum over the length of the barrel to improve the density and performance of the composite energetic material. Additionally, a screw was employed that had been optimized for the particular propellant formulation used in this investigation.

III.b Ingredients

The ingredients used in this investigation were for a nominal propellant formulation known as IH-AC3, given in *Table I*. It is a rocket propellant selected because it was an extruded composite energetic material for which there was a great deal of familiarity with processing in a TSE. The processing of IH-AC3 is extremely complex, requiring the use of the greatest number of feed streams of any formulation that has been continuously processed at NAVSEAIHMD, but is offset by the advantage that no development time is required for qualifying the formulation in the extrusion facilities. While the ingredients in Table I are nominal, the ammonium perchlorate concentration will be varied in this investigation through the range of 0.79 to 0.87 weight fraction. The nominal coarse-to-fine ratio was 70/30 as shown in the table, however the ratio of the coarse particle fraction to the fine particle fraction can range

from 50/50 to 81/19. It is the exploration of this region of the material design space that will be of interest in the combinatorial approach presented here.

III.c Determination of shape factor, delay parameter, and order of the mixing model

In the early 1990s, a Navy continuous processing project used fiber optic probes mounted in the process section and die to detect the presence and concentration of a blue dye in the process stream. The calibrated microencapsulated sensor (CAMES) instrumentation, or CAMES probe as it has come to be known (*Figure 2*), was custom built by MACH I, King of Prussia, PA. It operates on the principal of absorbed and reflected light and consists of a bifurcated optical fiber with a tuned LED source and highly sensitive photomultiplier. Because the formulation is colored a deep red due to the concentration of highly absorbing iron oxide, a concentrated organic blue dye was used for the RTD studies. The dye was Automate™ Blue 8A liquid dye from Rhom & Haas Co., Philadelphia, PA. It is a solution of mixed dyes in predominately xylene. One gram of the solution was added to a small mixture of the filler, a viscous polybutadiene resin, and fumed silica to form a semi-soft pill to drop into the solids feeding port of the extruder.

For processing of energetic materials in the TSE, it is essential that the addition of dyes be conducted remotely using an in-house designed rotating table. Before the device could be used with propellant, it had to be used once in a full operation with an inert formulation as required by NAVSEAIHMD safety regulations. The data was acquired using a PLC-based supervisory control system at the slow rate of 1 Hz. There was no capability for higher acquisition rates without adding specialized equipment. The signal

did not contain noise or oscillations in the signal. Therefore, post filtering of the signal was unnecessary.

The shape factor, delay volume, and order of the mixing model for a best fit of equation (2) to the RTD data for the two extreme concentration conditions of 79 and 87 wt. % RTD of interest in this investigation are given in *Table II*. Comparisons of the optical measurements with the fits from equation (2) for these two extreme compositions can be seen in *Figure 3*. All of the parameters are very similar, indicating that the response of the TSE response is independent of composition. This is a very important finding for using equation (1) in the combinatorial approach, since it indicates that a single value of each parameter can be used for predicting the gradient architecture that evolves over a wide composition range.

III.d Gradient Architecture Fabricated Using Twin Screw Extrusion Processing

Once the parameters for the convolution process model had been determined, it was possible to predict and fabricate energetic materials over a range of compositions for the combinatorial approach. To verify this combinatorial approach, a gradient architecture was fabricated using a step change in composition to the input of the extruder. Optical measurements of the gradient architecture can be seen in *Figure 4*, along with the predictions from Equation (1) using the parameters determined from the RVD measurements. It has been shown previously that the composition is directly related to the measurement signal [1]. Therefore, the composition could be determined as a function of position in the extrudate as seen in *Figure 5*. For gradient architectures, it is conventional to describe the composition variation using a simple polynomial or power law description [5]. A typical power law description is as follows:

$$V(x) = (V_1-V_0)*(x/t)^p+V_0 \quad (4)$$

Where $V(x)$ is the volume fraction at position x, V_0 is the volume fraction at $x = 0$, V_1 is the volume fraction at $x = 1$, t is the interlayer thickness of the gradient architecture, and p is the gradient exponent. The value x/t provides the relative position within the interlayer of the gradient architecture. For the TSE processed polymer composites, a gradient exponent of 0.5 over a length of 10 cm adequately describes the variation in composition up until the region of nearly constant composition in Figure 5 for the combinatorial approach. It is this region of the extrudate that will have burning rate properties characterized for the purposes of the combinatorial approach. Alternatively, it was determined that the following exponential formula could provide an accurate description for the gradient architecture extending well into the region of nearly constant composition [1]:

$$V(x) = a+b*exp(-xn) \quad (5)$$

where a is the value at the far extreme of the gradient, b is the change in volume fraction through the gradient, and n is the gradient exponent. In this formula, the absolute position x can be used instead of a relative position in the power law description.

While the optical probe utilized in this study was unique to the TSE facility where the energetic material was fabricated, it was also possible to use standard pressure and torque transducers to monitor the TSE process during the fabrication of the gradient architecture. These measurements are shown in *Figure 6*. While the pressure transducer measurements were fairly well predicted by Equation (1), the torque measurements required using a value for the order of the mixing process that was 1 less

than that determined from the residence distribution experiments. This may be understandable since there may be an additional effect of the mixing process between the end of the screw and the exit from the die. In both cases, there was some overshoot observed that stablized out after 75 seconds. Neglecting this overshoot, it should be viable to use either measurement to predict the composition variation in the TSE process for the combinatorial approach.

III. Characterization of Burning Rate Properties Over Composition Range For Combinatorial Approach

IV.a Acoustic Strand Burner Test Description

The best measure of a propellant's combustion properties is to test it in a motor; however, this is costly and inefficient during development. Instead, a good alternative is to conduct strand burning tests under a range of conditions (e.g., chamber pressure and temperature). Testing at different pressures allows determination of the burning rate exponent. The common method of strand burning is to test six-inch long strands ¼-inch in thickness and report the average burning rate for approximately six strands. Two thin tin bridge wires are inserted through the strand after the ignition point and before the end. The distance and time between wire failure is used to estimate the burning rate. The accuracy of the method is >> 1 percent.

The dynamic burning rate of a functionally graded propellant was characterized using an acoustic strand burner [6]. Employing a microphone in the combustion chamber, it is typically more accurate than using wires. Because of the variation in burning rate through the gradient architecture, a test plan had to be formulated for extracting specimens from the graded strands. The acoustic strand burner test unit was

modified to accommodate one pair of bridge wires to measure the mechanical burning rate as well for additional sampling. The system was also modified to allow testing of smaller lengths to minimize the variation in burning rate. Eventually it was found that strand segments as short as 2 to 3 inches could be tested. The distance required between bridge wires limited their use to the 3 inch specimens. The general sectioning scheme and bridge wire placement strategy for a typical set of four graded strands is shown in *Figure 7*. The plan allowed for the fourth strand to be used in case of a misfire. A photograph of a set of test specimens with igniters and bridge wires in place is shown in *Figure 8*. Strands obtained near the central axis of each specimen segement were submitted for acoustic burning rate testing. These are identified as strands 1 through 4 as shown in *Figure 9*.

IV.c Acoustic Strand Burning Test Results and Interpretation

Once the capabilities of the acoustic test unit and the strand test strategy were settled, testing proceeded smoothly with minimal failures of the mechanical bridge wire measurements. The measured burning rate data for one set of four strands sectioned into six test specimens, as illustrated in Figure 7, are plotted in *Figure 10*. In that particular test series, there were two failures of the bridge wire measurement. Therefore only two *mechanical* points were plotted in Figure 10 instead of four. Because the test method of notching the strands at close intervals was changed after they had been cut, there was not enough length before the gradient to verify the initial homogeneous composition. These data will be sought in the future. For reference, the ranges of experimental burning rate measurements for the 87 and 79 percent homogenous compositions are shown in Figure 10.

Figure 11 illustrates clearly how the sectioning strategy was used to characterize the gradient; only data from a single grain is shown for clarity. The best approach to interpret the data is to consider the measurements as moving averages. For example in Figure 11, the bars are not any uncertainty but rather represent the length over which the average was taken. The mechanical burning rates (from the tin bridge wires) were treated as a moving average over a slightly shorter distance, though the technique not was as accurate as the acoustic measurements and were subject to higher variance.

The negative gradient in AP content was characterized by taking central strands from two extruded grains (designations TDF, VDB, etc. were for identification purposes) at locations offset by two inches. There was good agreement between the two grains as shown in *Figure 12*, and offsetting the sampling extended the range of characterization providing verification where the two overlapped. In the future a longer offset distance will be employed.

The grains that were processed with a positive gradient were sampled quite differently. An error in grain identification during cutting resulted in four positive gradient grains being sampled. All samples were submitted for testing to verify repeatability of gradient architecture. It was found that the repeatability was very satisfactory. The acoustic burning rate data from the positive gradient strands are plotted in *Figure 13*. The mechanical measurements of burning rate agreed well and complemented the acoustic measurements. These data are also plotted in Figure 13.

The response in AP content of extruded propellant to a step change in AP feeding rate during twin-screw extrusion can be predicted using process models based on Equation (1). The zero inches reference point in Figures 11 and 12 were actually 14.875

inches from the leading end of the extruded grain. Using this and a value of 7.92 cm^2 for the cross-sectional area of the die, location was transformed into volume extruded. The burning rate responses for the positive step change were normalized to range from zero to one. The resulting transformation is plotted in Figure 5-41.

There was interest in understanding if the step change in the positive and negative directions could produce the same gradients. Comparing the burning rate data from the strand burning tests, seen in *Figure 14*, the combustion properties for each gradient architecture appear to have slightly different spatial gradients. This is not a problem since Equation (1) is capable of predicting the gradient architecture for both positive and negative step changes, as seen in *Figure 15*. This has important implications in the combinatorial approach, since it will not be necessary to go back to the original feed rate condition in order to generate the next gradient architecture. Therefore, in the production of graded composites using the TSE process, these results indicate that gradient architectures can be simply and continuously varied to minimize waste and produce property data over a wider range of formulations.

V. Comparison of Compositional Dependence from Combinatorial Approach with Compositional Dependence Using Kowalski Algorithm

It was desirable to compare the compositional dependence of properties from the combinatorial approach with a conventional approach for ascertaining the effects of the individual ingredients on the burning rates as produced over the range of feeding and extruding capability for the process. Designed mixture experiment methodology was recognized as the most efficient and thorough method to achieve this goal. This family of methods can quantify the contribution of individual ingredients and more importantly

the combined effects of two or more ingredients using response surface analytical methods. Most mixture designs are based on component proportions and not total quantity of a mixture. This is the situation for the composite propellant; the burning rate is a function of the relative amounts of ingredients and not propellant quantity.

Manufacturing IH-AC3 using the continuous process is more efficient, more environmentally benign, and cost effective compared to the batch process. However, preparing a number of propellant samples remotely at a wide variety of compositions and process conditions is nevertheless an expensive and complex undertaking. While this is the usual route for any propellant development or characterization study, following a designed method will ensure the most viable (and defendable) data and results possible. These facts have been widely recognized, and these methods have been applied to continuous processing at Navy facilities for some years.

V.a Kowalski-Cornell Algorithm

Kowalski and Cornell suggests a Taylor series approximation for the process variables which best suits response surface analyses [7]:

$$\eta_{PV}(z_k) = \alpha_0 + \sum_{k=1}^{n} \alpha_k z_k + \sum_{k=1}^{n} \alpha_{kk} z_k^2 + \sum \sum_{k<l}^{n} \alpha_{kl} z_k z_l \tag{6}$$

Equation (6) can be be combined with the following:

$$\begin{aligned} \eta(\vec{x}, \vec{z}) = & \sum_{i=1}^{q} \beta_i x_i + \sum \sum_{i<j}^{q} \beta_{ij} x_i x_j + \sum_{i=1}^{q} \sum_{k=1}^{n} \gamma_{ik} x_i z_k \\ & + \sum_{i=1}^{q} \sum \sum_{k<l}^{n} \gamma_{ikl} x_i z_k z_l + \sum \sum_{i<j}^{q} \sum_{k=1}^{n} \gamma_{ijk} x_i x_j z_k \\ & + \sum \sum_{i<j}^{q} \sum \sum_{k<l}^{n} \gamma_{ijkl} x_i x_j z_k z_l \end{aligned} \tag{7}$$

to yield a second-degree model:

$$\eta_{PV}\left(\vec{x},\vec{z}\right)=\sum_{i=1}^{q}\beta_i x_i+\sum\sum_{i<j}^{q}\beta_{ij}x_i x_j+\sum_{k=1}^{n}\alpha_{kk}z_k^2+\sum\sum_{k<l}^{n}\alpha_{kl}z_k z_l+\sum_{i=1}^{q}\sum_{k=1}^{n}\gamma_{ik}x_i z_k \tag{8}$$

This model includes the mixture model with a pure quadratic that has a two-factor interaction effects among the process variables, a two-factor interactions between the linear blending terms in the mixture (constituents), and the main effect terms in the process variables. This model requires a design size of $(q+n)(q+n+1)/2$ points. It requires less design points for fitting than Equation (6), and the quadratic terms can be omitted if not necessary further reducing the design points. Kowalski describes a process for constructing the new design. However a description of the factors for the IH-AC3 experiment is necessary. The goal of the experiment should dictate the design. To do otherwise is to limit one's success and quite possibly introduce bias.

V.b Mixture/Process Experiment for IH-AC3

There were a number of reasonable process constraints that were identified and incorporated in the design strategy. The ingredients for the propellant were fed to the extruder as blends and mixtures, so the blends were treated as the factors or constituents for the mixture matrix (not the individual ingredients). There were two other constraints to consider. The first was a consideration of the established process methodology for this formulation and the possible strategies for achieving gradient structures in the extrudate within those methods. The other consideration was the ingredient ranges imposed by any particular mixture design. For example some candidate experiment designs required combinations of feeding rates that could not be accommodated

economically or safely. These issues were studied exhaustively by the author and concluded satisfactorily.

Suffice to say that gradient control was confined to the two AP feedstreams. While this strategy unfortunately ignored the known influence of the modifiers, there was still enough flexibility with the AP feed streams to yield a significant effect in the burning rate. Given these constraints, the burning rate is influenced by overall concentration of AP as defined by its converse, the concentration of binder. Additionally, it is also influenced by the ratio of coarse to fine AP particles. This was expressed as the individual concentrations of AP grind fractions for the sake of the mixture experiment. Finally, this experiment represented the best opportunity to settle a longstanding uncertainty, i. e., experiment observations that suggested extruder screw speed may influence the burning rate. Therefore the mixture and process experiment included three mixture factors and one process factor, the ranges and levels respectively are given in *Table III*. The processing conditions identified by the Kowalski-Conner algorithm are shown in *Table IV*.

V.c Results of the Extrusion Trials and Strand Burning Rate Data

All combinations were produced using the 40 mm twin-screw extruder. Small *strands* of propellant measuring ¼ x ¼ x 6 inches were cut for strand burning rate test [6]. Complete characterization of the burning rate dictates that the strand testing be conducted over a range of temperatures and operating pressures, since the burning rate is dependent upon the test conditions. However this was a technology program and not a propellant development program, so testing was conducted at one temperature—ambient. This is a typical approach by propellant formulators for screening large sets of

strands. Since the graded motors were to be designed with a relatively low operating pressure, the strands were tested at 500, 1000, and 1500 psig chamber pressures. The average burning rate for each mixture and process combination is also presented in *Table IV*. The design space yielded a satisfactory range of burning rates. The range approximately doubled at the higher test pressures despite the conservative processing and feeding constraints.

V.d Analysis and Interpretation of the Burning Rate Data

A rigorous response surface analysis was conducted for the burning rate data according to methods proposed by Kowalski and Cornell, as well as Piepel and Cornell [7,8]. The mixture points were expressed in terms of the actual yields of coarse and fine particles as in *Table IV* where,

x_1 = fraction of coarse 90 μm Ammonium Perchlorate
x_2 = fraction of fine 10 μm Ammonium Perchlorate
x_3 = fraction of binder including modifiers
z_1 = extruder screw speed (RPM)

Because upper (and lower by implication) bounds were used to constrain the mixtures, the constituents were converted to *u*-pseudocomponents [9]. Therefore the u-pseudo-components were,

$$u_i = \frac{U_i - x_i}{\sum_{i=1}^{q} U_i - 1} \tag{9}$$

where,

U_i = the upper limit of the i^{th} component

then, for the number of mixture components, $q = 3$,

$$u_1 = \frac{0.7041 - x_1}{0.3257} \tag{10}$$

$$u_2 = \frac{0.4116 - x_2}{0.3257} \tag{11}$$

$$u_3 = \frac{0.2100 - x_3}{0.3257} \tag{12}$$

Equation (8) was tested against the *u*-pseudocomponents for each chamber pressure using step-wise regression and analysis of variance, where the equation is expressed in terms of the pseudocomponents as follows:

$$\eta_{PV}(\varpi \varpi) = \eta_{PV}(3,1) = \beta_1 u_1 + \beta_2 u_2 + \beta_3 u_3 + \beta_{12} u_1 u_2 + \beta_{13} u_1 u_3 + \beta_{23} u_2 u_3 + \alpha_{11} z_1^2 + \gamma_{11} u_1 z_1 + \gamma_{21} u_2 z_1 + \gamma_{31} u_3 z_1 + \varepsilon \tag{13}$$

Equation (12) was tested against the *u*-pseudocomponents for each chamber pressure using step-wise regression and analysis of variance. Conditions *I* (the centroid point at 65 rpm) and *P* (an extra point to check the fit of the model) were excluded from the model analysis. The analysis of variance was conducted step-wise using a significance of α = 0.10; however the results were down-selected to alpha values of much less. This enabled the coefficients to be determined in Equation (13) for constructing the response surface for the burning rate data.

V.e Response Surface Analysis Burning Rate Data

The corresponding models given by the parameters in Equation (13) were used to generate the response surface curve for comparison with the results from the combinatorial approach (*Figure 16*). The predictions for an extruder speed of 85 rpm were of most interest because that speed was to be used to make the graded propellant. The contours indicate the predicted burning rate for that screw speed and many ingredient combinations. The plotted points are the experimental burning rates for that combination and screw speed. Because of the complexity in conveying a three variable

function as a two-axis contour plot, only the solids fraction is readily identifiable in the Figure 16. The top line in each diagram represents 13 percent binder or the highest level of AP tested. The AP fractions were best interpreted as the ratio of coarse to fine. As one moves from left to right across the figures the coarse to fine ratio is decreasing, i. e., the relative amount of fine particles is increasing. The dotted line in the left hand side of each figure represents a coarse-to-fine ratio of 79/21. At the opposite side, the ratio is 50/50 for the rightmost vertex. The ratio passing through the centroid is approximately 63/37. It is the coarse-to-fine ratio of 79/21 represented by the dotted line in Figure 16 that was used for creating the gradient architecture for the combinatorial approach.

Comparison of the burning rates versus composition for the new combinational approach and the design of experiments can be seen in *Figure 17*. The compositions in the combinatorial approach were determined using the power law gradient architecture determined in Figure 5. From these comparisons, it is clear that the new combinatorial approach is capable of reproducing the compositional dependence of the energetic materials that was produced by the conventional design of experiments.

VI. Conclusions

A combinatorial approach based on Twin Screw Extrusion has been developed for evaluating new composite energetic materials. Materials with gradient architectures are produced by the TSE process. The combinatorial approach uses a convolution process model to predict the variation of composition in the gradient architecture. Experiments were developed for characterizing the variation in burning rate through the gradient architecture using strand burning tests. Comparisons of the burning rate dependence on composition from the new combinatorial approach were made with

results from a more conventional design of experiments. Both sets of results were in good agreement verifying the applicability of the combinatorial approach to developing new composite energetic materials. Because the TSE process is used to manufacture both energetic and non-energetic composite materials, the combinatorial approach can also be applied to the development of new polymer composites for non-energetic applications.

VII. References

[1] Gallant, F.M., Bruck, H.A., and Kota, A., (2004). "Fabrication of Particle-reinforced Polymers with Continuous Gradient Architectures Using Twin Screw Extrusion Processing", to appear in *Journal of Composite Materials*.

[2] Gallant, F. M. (2000). Continuous Extrusion of EX-101 Gun Propellant--A Green Munition. Indian Head, MD, Naval Surface Warfare Center Indian Head Division**:** 30.

[3] Gallant, F. M., W. Newton, et al. (1999). Feeding Performance Studies for CPOCP Program Ingredients. Indian Head, MD, Naval Surface Warfare Center Indian Head Division**:** 41.

[4] Newton, W., F. M. Gallant, et al. (1999). Preblending and Feeding Strategies for the Continuous Processing of Extruded Composite Propellant. Indian Head, MD, Naval Surface Warfare Center Indian Head Division**:** 30.

[5] Markworth, A.J., Ramesh, K.S., and Parks, W.P., Jr. (1995). "Review: Modelling Studies Applied to Functionally Graded Materials", *Journal of Materials Science*, **30**, 2183-2193.

[6] Rampichini, S., Ruspa, D., and DeLuca, L.T. (2000). Acoustic Emission of Underwater Burning Solids Rocket Propellants. Combustion of Energetic Materials. K. K. Kuo and L. T. DeLuca. New York, Begell House, Inc.

[7] Kowalski, S. and J. Cornell (2000). "A new model and class of designs for mixture experiments with process variables." Communications in Statistics-Theory and Methods **29**(9&10): 2255-2280.

[8] Piepel, G. F. and J. A. Cornell (1994). "Mixture Experiment Approaches: Examples, Discussion, and Recommendations." Journal of Quality Technology **26**(3): 177-196.

[9] Crosier, R. B. (1986). "Mixture Experiments: Geometry and Pseudo-Components." Technometrics **26**: 209-216.

Table I. Nominal formulation for IH-AC3 rocket propellant.

Ingredient	Weight Percentage	Function
Ammonium perchlorate (90 μm)	58.8	Oxidizer
Ammonium perchlorate (10 μm)	27.2	Oxidizer
Zeon Chemical HyTemp® 4404	7.92	Binder
Dioctyl adipate	5.00	Plasticizer
3M Dynamar® HX-752	0.32	Bonding agent
Isophorone diisocyanate	0.26	Curative
Graphite	0.50	Extrusion aid
Zirconium carbide	0.50	Combustion modifier
Iron oxide	1.50	Ballistic modifier

Table II. RTD data for IH-AC3 rocket propellant at extreme concentrations

Wt. % AP	Delay Volume, v_d (liters)	Order of Model	Shape Factor, a_v	95% CI for Shape Factor	Sum Squares Residuals
87.0	0.235	4	43.23	±0.59	25.12
79.0	0.237	4	51.77	±0.55	45.41

Table III. Factors influencing burning rate of IH-AC3 propellant

Ingredient	Type	Range/Levels
AP Coarse Particle Grind (APC)	Mixture	40.3-70.4 % by weight
AP Fine Particle Grind (APF)	Mixture	16.6-41.2
Binder (BIN)	Mixture	13.0-21.0
Extruder Screw Speed (RPM)	Process	45 and 85

Table IV. The Individual Test Combinations and Average Burning Rates (Sorted by Fines) of the Homogeneous Propellant Strands.

			Effective Yields			Avg. Burning Rate for Test Pressure (psig)		
ID	**Point Type**	**RPM**	**Coarse**	**Fines**	**Binder**	**500**	**1,000**	**1,500**
L	Vertex	45	0.624	0.166	0.210	0.443	0.580	0.625
N	Vertex	45	0.704	0.166	0.130	0.630	1.085	1.460
P	Test Fitness	85	0.664	0.176	0.160	0.536	0.802	0.975
J	Edge centroid	85	0.514	0.277	0.210	0.526	0.735	0.773
K	Edge centroid	85	0.581	0.289	0.130	0.620	1.061	1.276
M	Edge centroid	85	0.664	0.289	0.170	0.513	0.731	0.834
F	Overall centroid	45	0.521	0.308	0.171	0.604	0.943	1.145
G	Overall centroid	85	0.521	0.308	0.171	0.546	0.799	0.915
H	Overall centroid	85	0.521	0.308	0.171	0.550	0.784	0.939
I	Overall centroid	65	0.521	0.308	0.171	0.601	0.899	1.072
A	Vertex	45	0.403	0.387	0.210	0.571	0.884	0.988
B	Edge centroid	85	0.408	0.399	0.193	0.609	0.854	1.001
C	Vertex	45	0.413	0.412	0.175	0.664	0.997	1.156
D	Edge centroid	85	0.436	0.412	0.153	0.666	1.006	1.272
E	Vertex	45	0.458	0.412	0.130	0.701	1.116	1.528

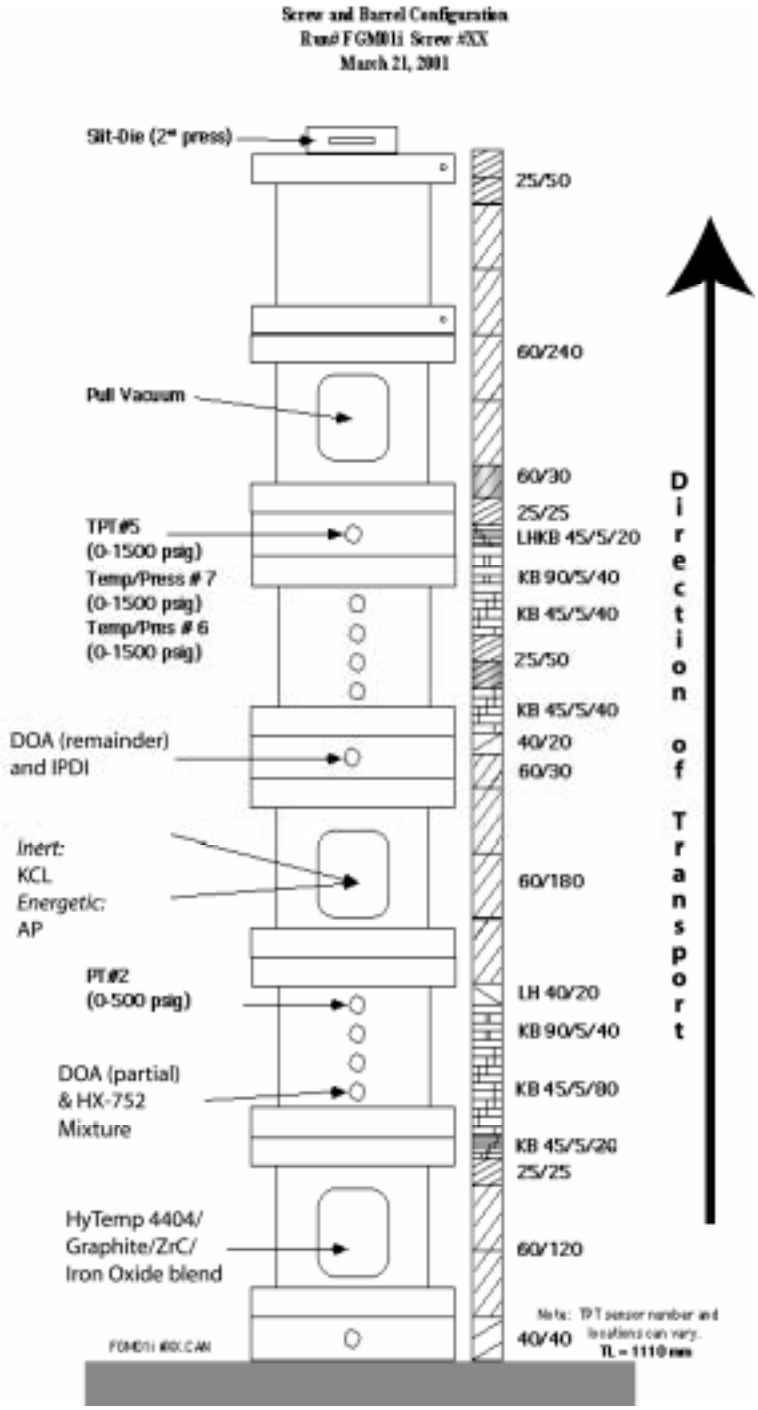

Figure 1. Extruder barrel configuration, screw design, feeding locations, and instrumentation sites for the ZSK-40 TSE at NAVSEAIHMD are illustrated. The Numbers next to the screw are for geometry descriptions, and TPT is a temperature-pressure transducer.

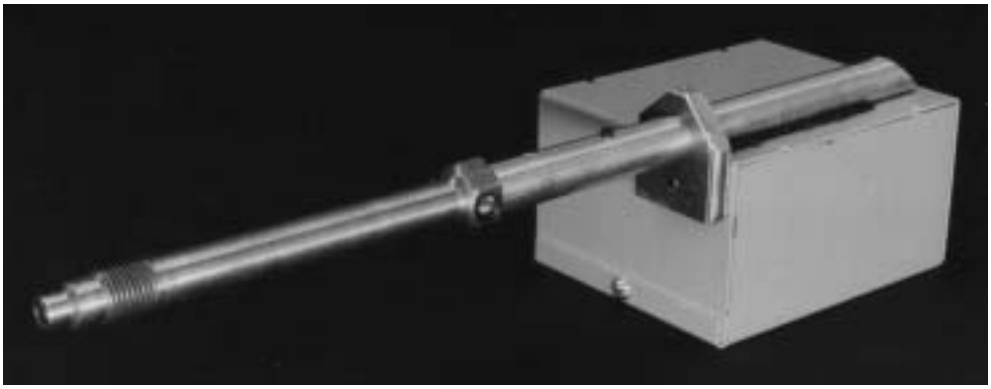

Figure 2. A fiber optic probe, referred to as the CAMES probe, was used at NAVSEAIHMD to detect concentration of tracer in RTD and other processing experiments

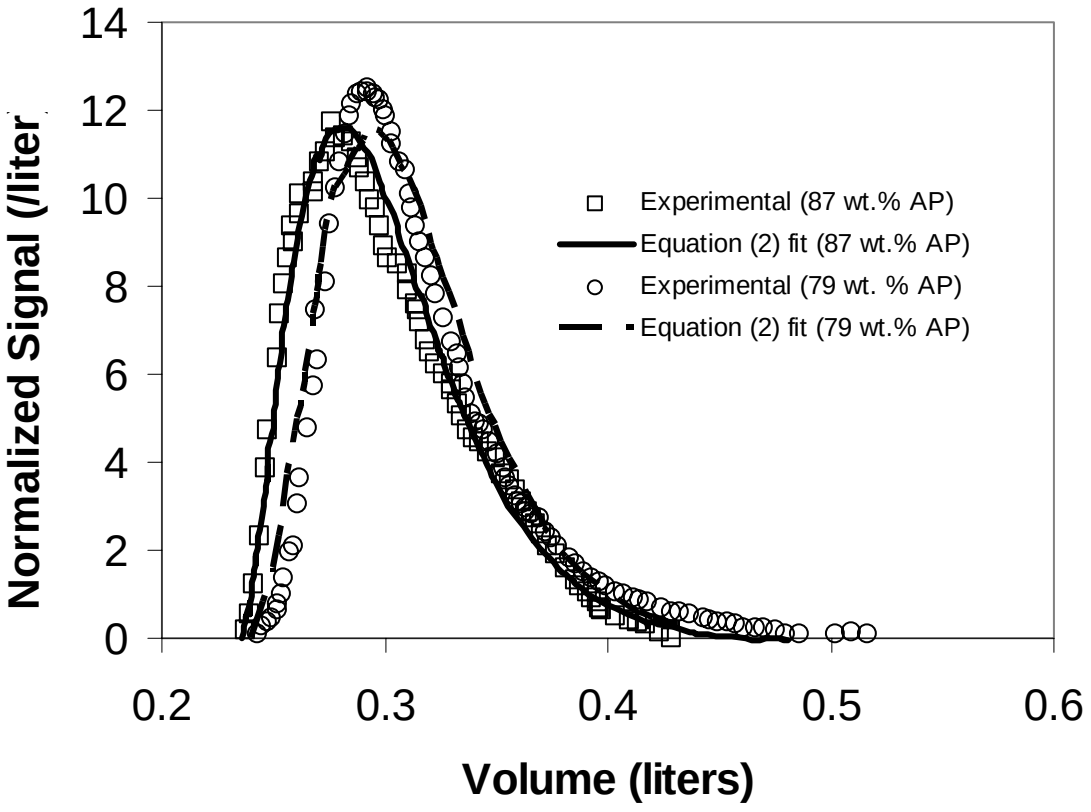

Figure 3. Optical measurements and fits from equation (2) used to determine parameters for TSE processing of IH-AC3 propellant at two extreme compositions

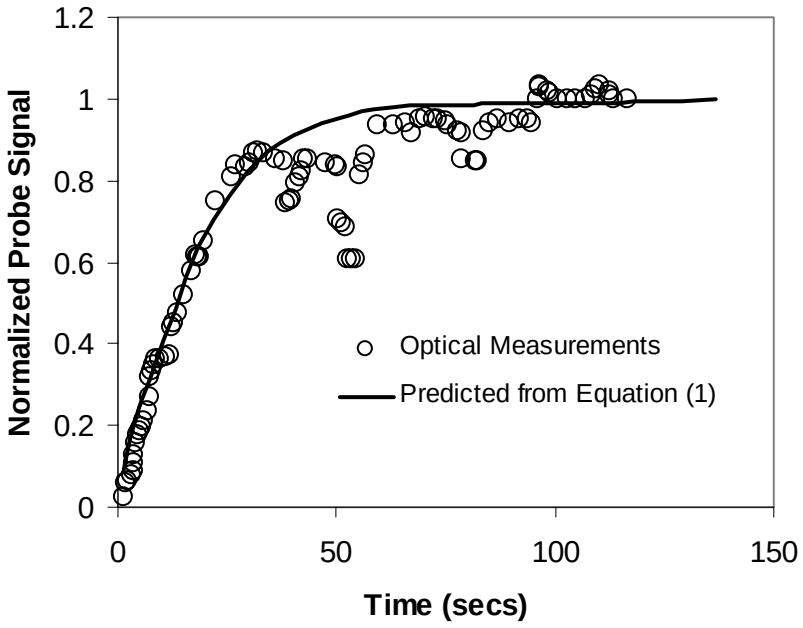

Figure 4. Optical measurement of gradient arcitecture output from the TSE for a step change to the input composition and gradient architecture predicted from equation (1)

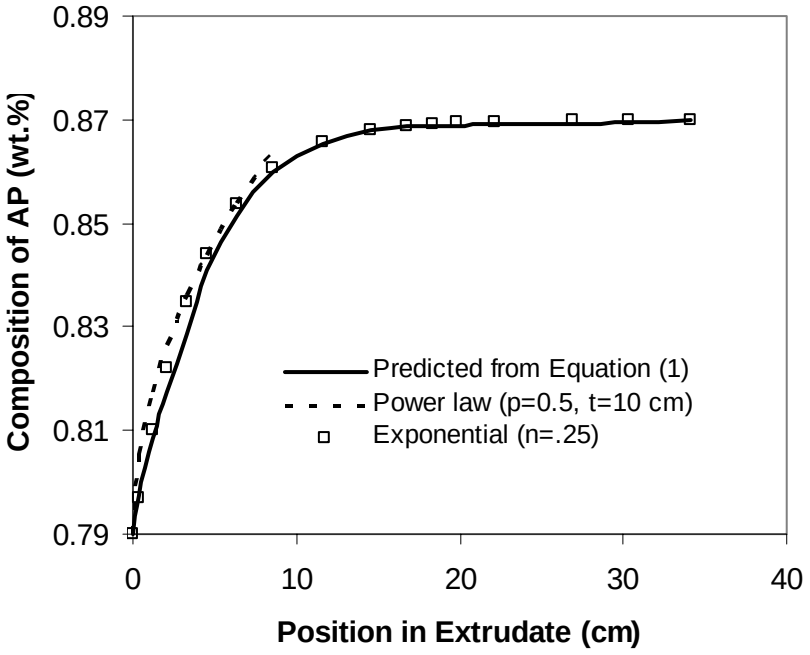

Figure 5. Variation of composition in extrudate, power law fit for a gradient exponent of 0.5 and interlayer thickness of 10 cm, and exponential fit with a gradient exponent of 0.25

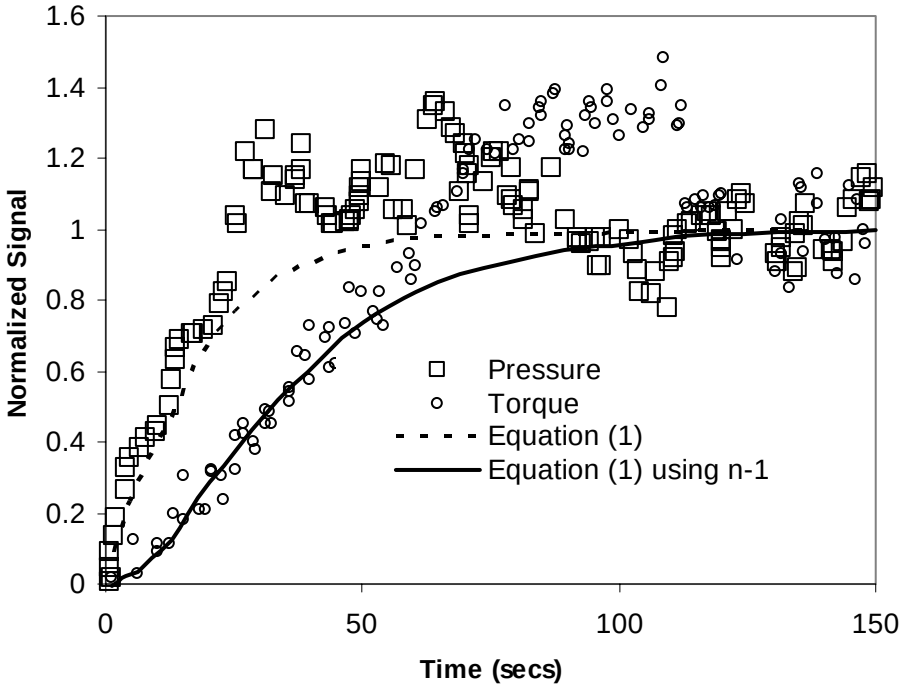

Figure 6. Pressure and torque transducer measurements of TSE process during step change to input compared with predictions using Equation (1).

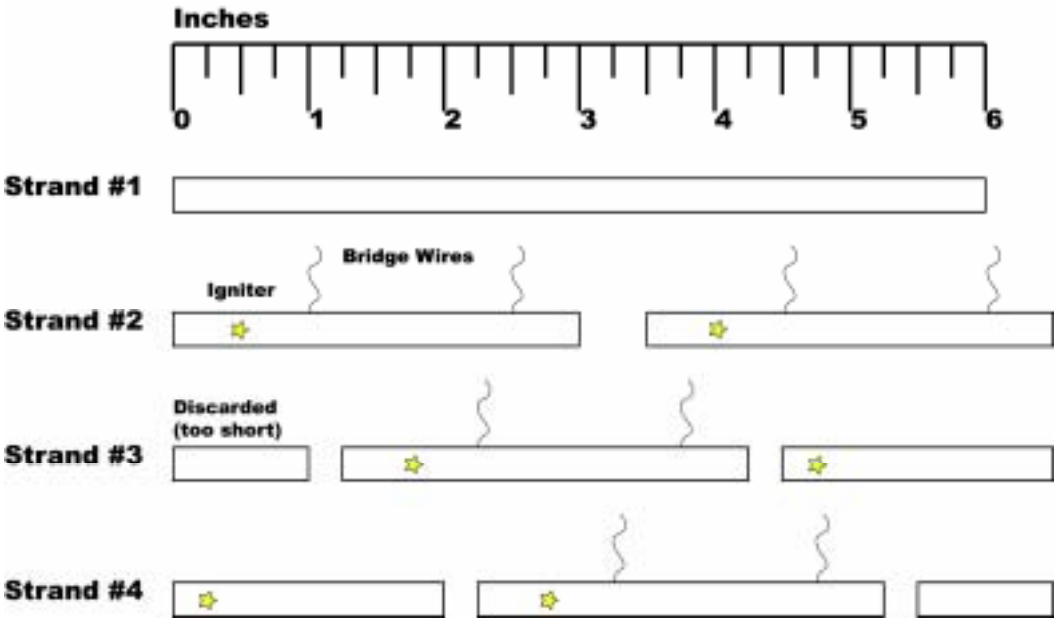

Figure 7. Test plan for characterizing burning rate of graded propellant in combinatorial apporach

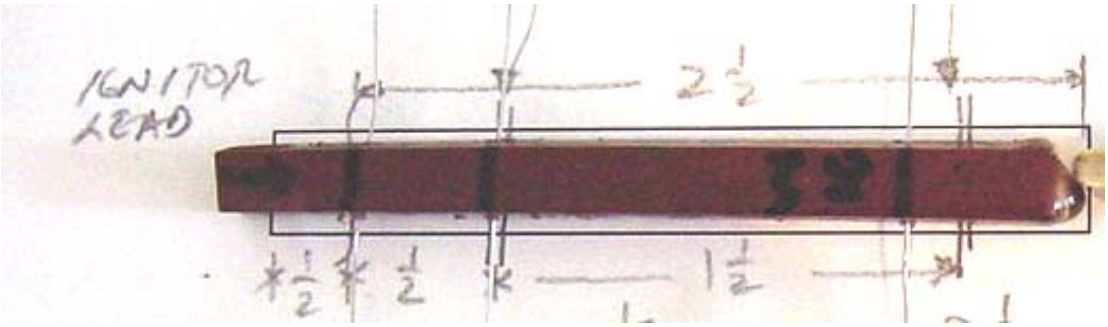

Figure 8. Typical 3-inch strand shown with igniter leads and bridge wires.

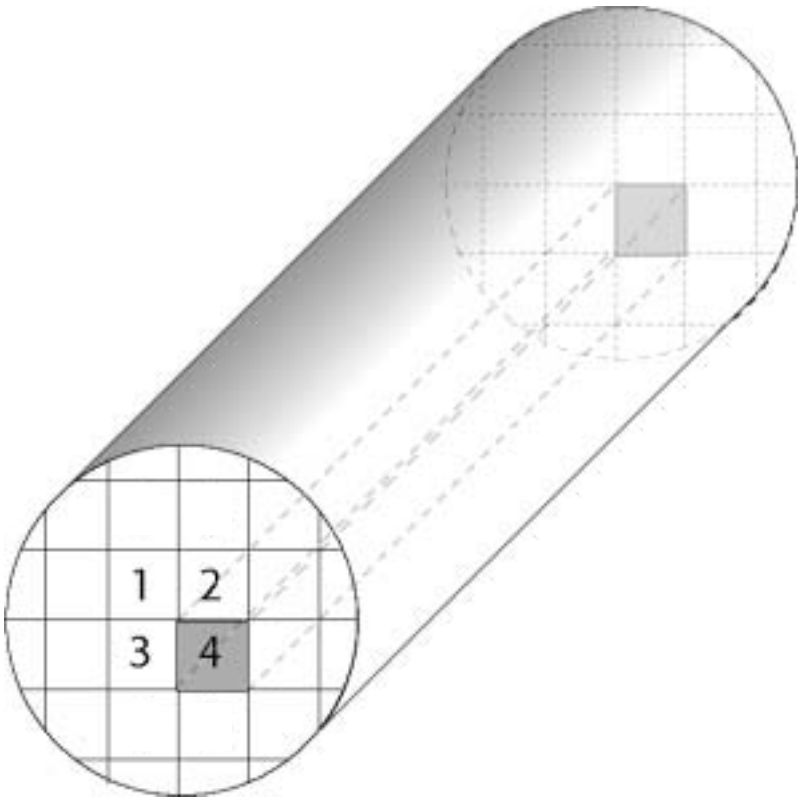

Figure 9. Four strands were obtained from each specimen segment according to the above scheme for burning rate testing.

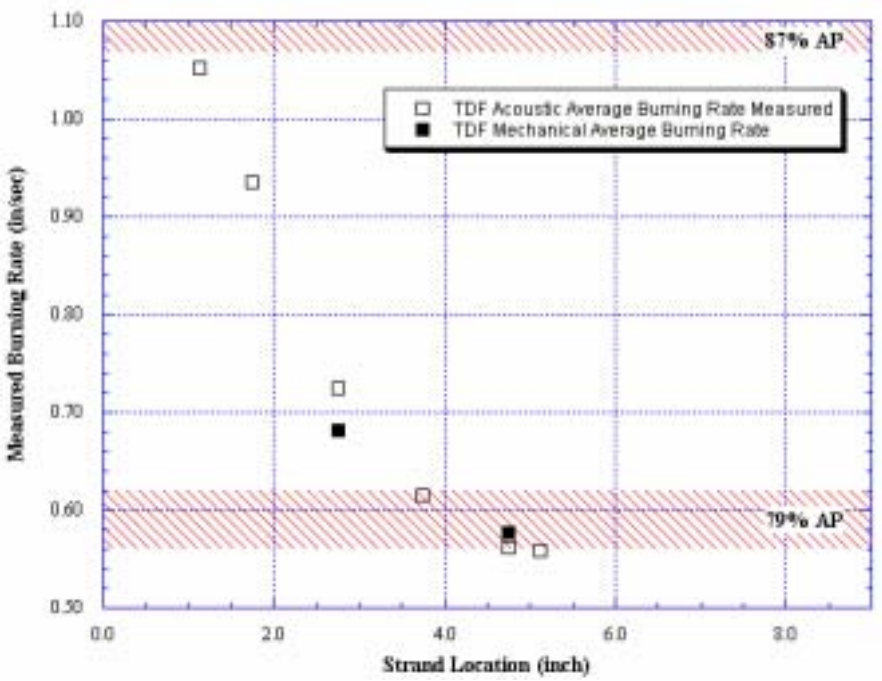

Figure 10. The masured strand burning rates for the six short strands taken from the center of a single functionally graded rocket grain were plotted. Burning rates were determined acoustically and electrically. The reference burning rate ranges for 87 and 79 percent AP are shown.

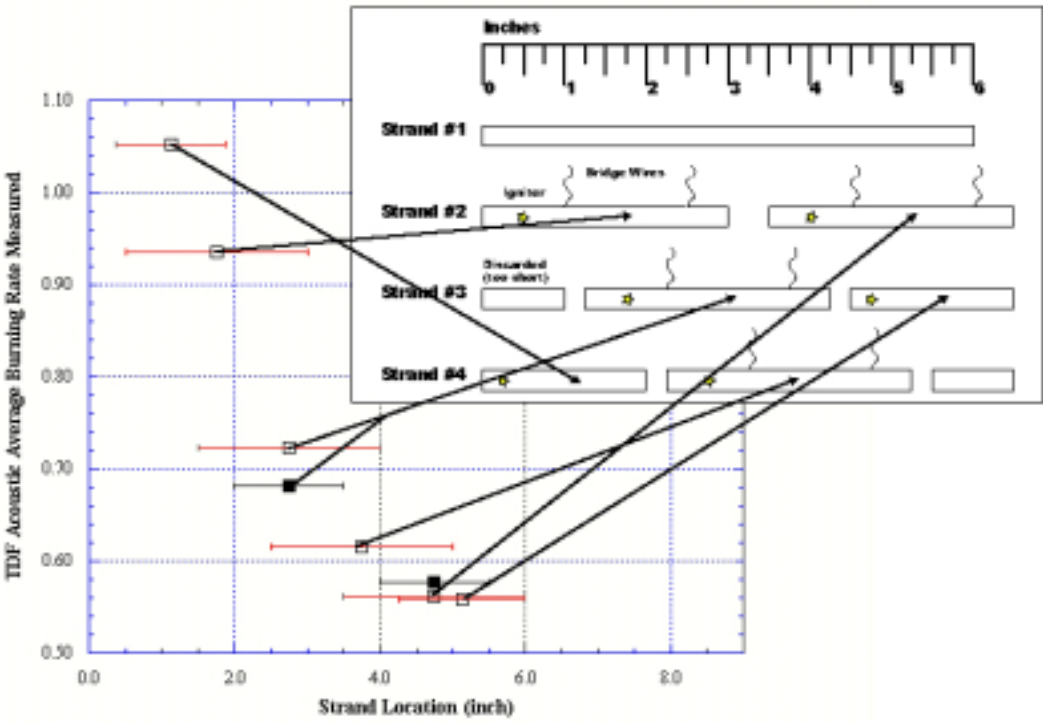

Figure 11. The bars on the plot represent the length over which the burning rate was determined—<u>not</u> uncertainty in location. The bars illustrate how testing of sequentially overlapping strands revealed the graded architecture.

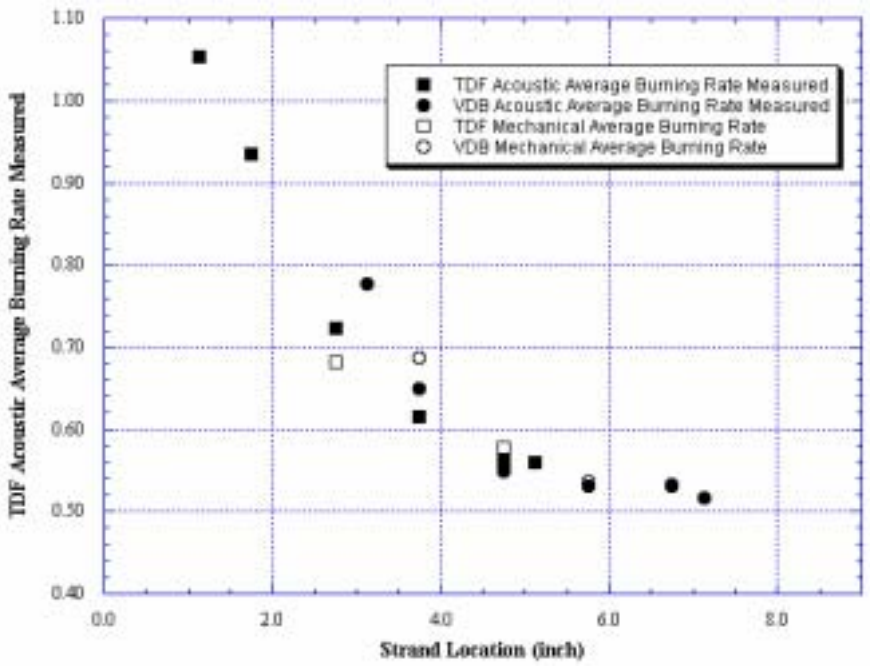

Figure 12. Strand burning rate results from two grains for negatively graded propellant.

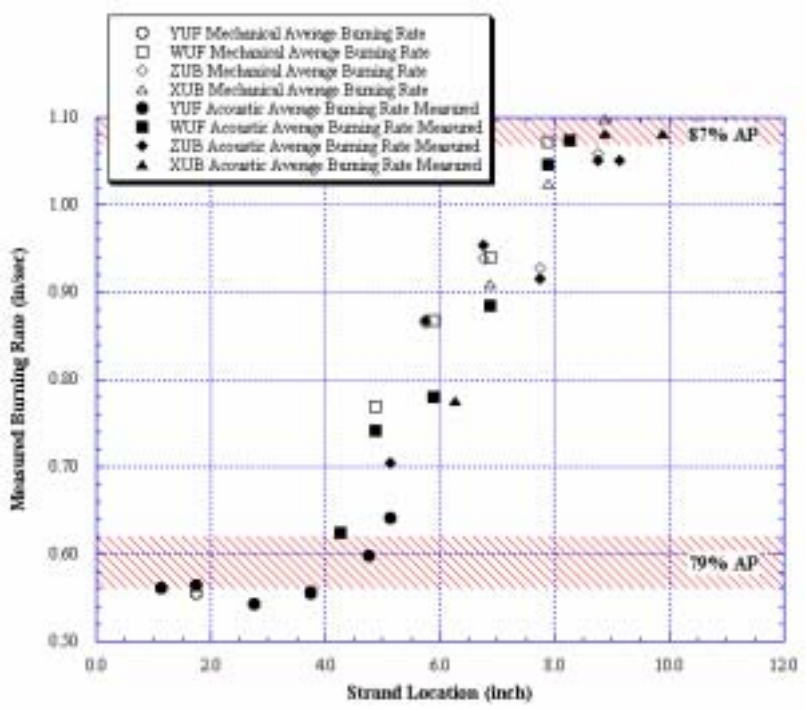

Figure 13. Mechanical burning rate measurements during the acoustic strand burning tests agree well with the acoustic responses.

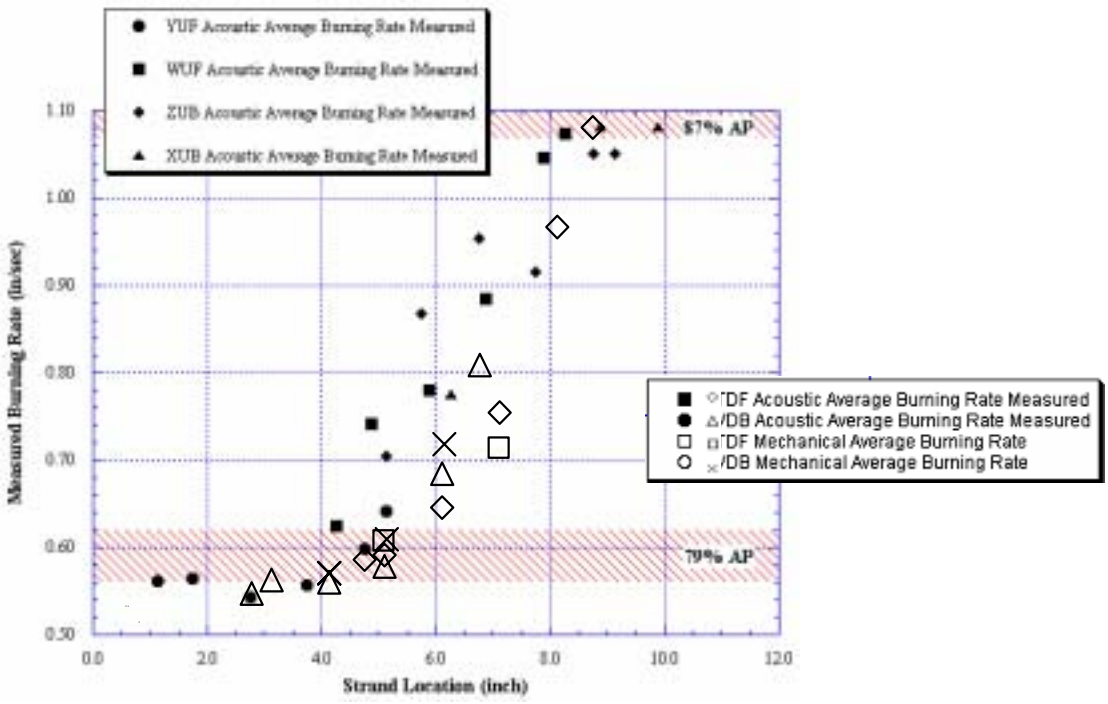

Figure 14. Comparison of the burning rate data from the strand burning testsfor positive and negative gradients indicating that gradient architectures are similar

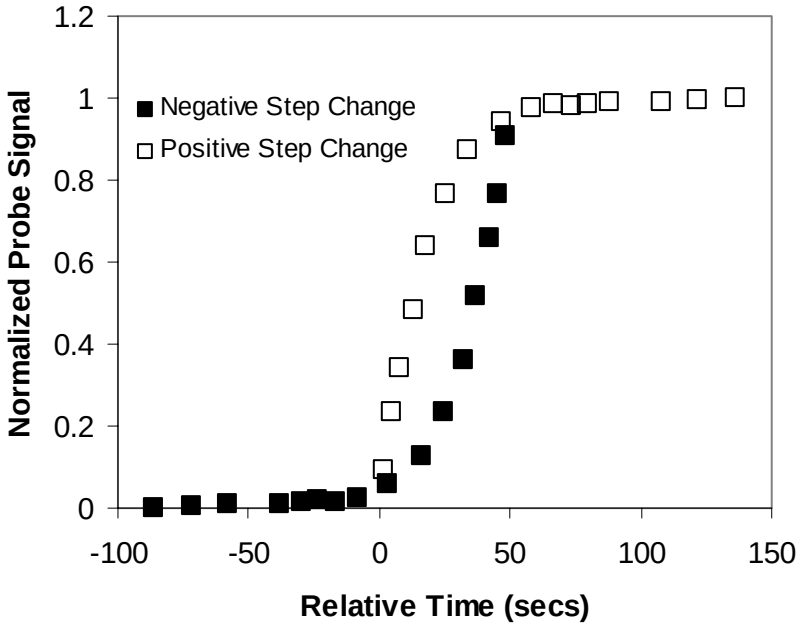

Figure 15. Comparison of spatial variations for positive and negative step changes in TSE input conditions predicted by Equation (1).

→→→→→Decreasing Coarse-to-Fine Ratio→→→→→

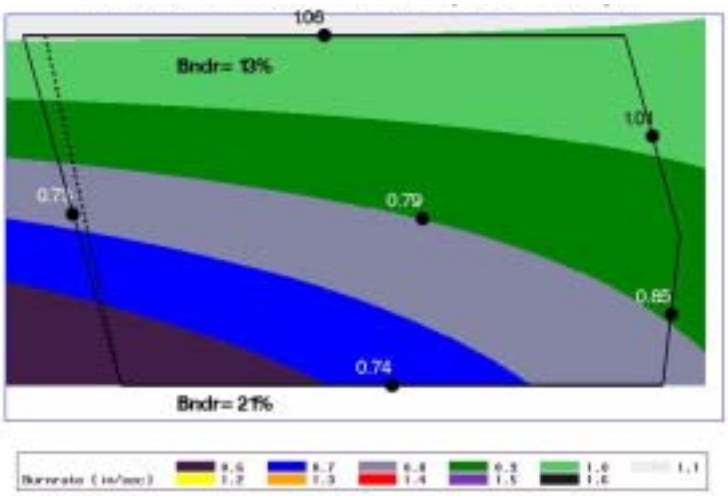

Figure 16. The results of the response surface analysis were plotted as a two-dimensional contour for a 1,000 psig condition and extruder speed of 85 rpm. The numbers are the experimental results.

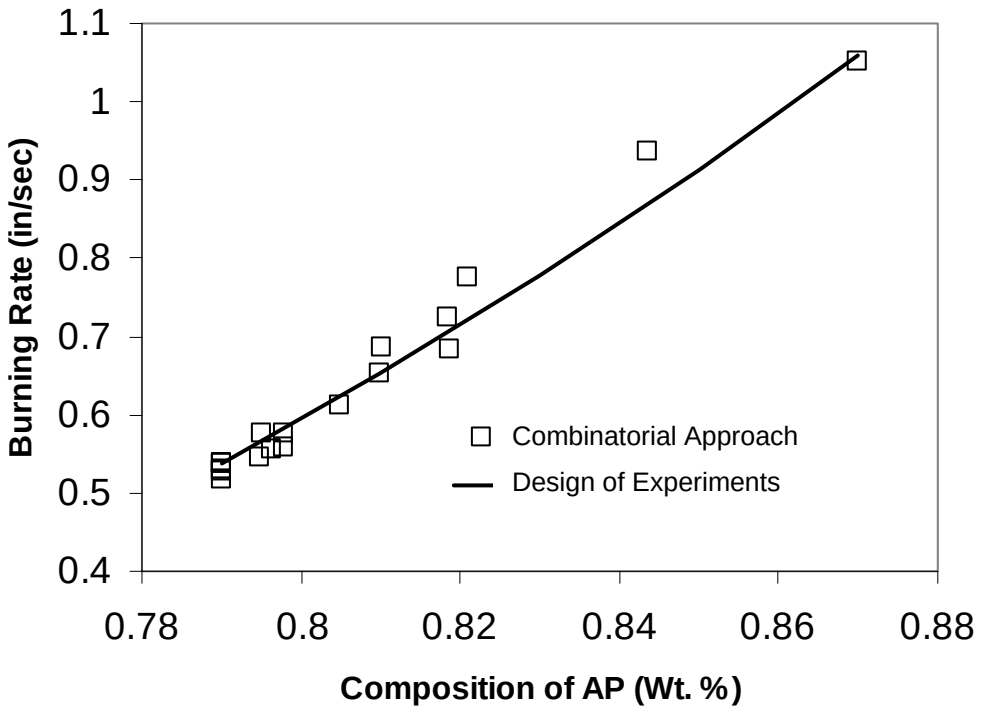

Figure 17. Comparison of burning rate versus composition from new combinatorial approach with variation determined by conventional design of experiments.